

# Structural and optical properties of polycrystalline CdS thin films deposited by electron beam evaporation\*

Yang Dingyu(杨定宇)<sup>†</sup>, Zhu Xinghua(朱兴华), Wei Zhaorong(魏昭荣), Yang Weiqing(杨维清), Li Lezhong(李乐中), Yang Jun(杨军), and Gao Xiuying(高秀英)

School of Optoelectronic Technology, Chengdu University of Information Technology, Chengdu 610225, China

**Abstract:** Highly crystalline and transparent cadmium sulphide (CdS) films were deposited on glass substrate by electron beam evaporation technique. The structural and optical properties of the films were investigated. The X-ray diffraction analysis revealed that the CdS films have a hexagonal structure and exhibit preferred orientation along the (002) plane. Meanwhile, the crystalline quality of samples increased first and then decreased as the substrate temperature improved, which is attributed to the variation in film thickness. UV-vis spectra of CdS films indicate that the absorption edge becomes steeper and the band gap present fluctuation changes in the range of 2.389–2.448 eV as the substrate temperature increased. The photoluminescence peak of the CdS films was found to be broadened seriously and there only emerges a red emission band at 1.60 eV. The above results were analyzed and discussed.

**Key words:** polycrystalline CdS thin film; substrate temperature; UV-vis spectrum; photoluminescence spectrum

**DOI:** 10.1088/1674-4926/32/2/023001

**PACC:** 8100; 6146; 8120

## 1. Introduction

Extensive research has been done on the deposition and characterization of cadmium sulphide (CdS) semiconductor thin films due to their potential application in the area of electronic and optoelectronic device. Polycrystalline CdS thin films are generally used in heterojunction solar cells as a window material for transmitting the light and also as the n-type material for p–n junction of the solar cells<sup>[1,2]</sup>. This material has been prepared by physical methods such as vacuum thermal evaporation<sup>[3]</sup>, sputtering<sup>[4]</sup> and chemical methods including spray pyrolysis<sup>[5]</sup> and chemical bath deposition (CBD)<sup>[6]</sup>. Compared with chemical methods, physical methods possess the advantages of convenience, high growth rate, and there is no wastewater discharge. Nowadays, the physical methods used for the preparation of CdS films have been seen as the developing direction to take the place of the traditional methods, such as CBD.

At present, the CdS films grown by the electron beam evaporation (EBE) technique have not been reported. In this paper, the hexagonal CdS thin films with excellent (002) orientation are successfully prepared by the EBE technique. It is well known that hexagonal CdS films invariably grow with columnar structure along the *c*-axis perpendicular to the substrate. This means that there are fewer grain boundaries parallel to the junction which would impede the flow of photogenerated excess carried to the grid<sup>[7]</sup>. The role of deposition temperature on the structural, optical properties of prepared samples has been investigated.

## 2. Experiment

The CdS thin films were deposited by electron beam evap-

oration at various substrate temperatures. The substrate holder was made of stainless steel and an array of tungsten–halogen lamps was used for substrate heating. A graphite boat was used as an evaporation boat and CdS pellets of 99.995% purity were used as the source material. The pellets were heated by electron beam for 3 min in a vacuum chamber (background vacuum is  $4 \times 10^{-3}$  Pa), and the electron beam intensity and energy were fixed at 30 mA and 6.5 keV. The source-to-substrate distance was maintained at 15 cm. During deposition of the CdS films, the substrate holder was rotated to improve the uniformity of the films. Borosilicate glass slides were used as substrates for the CdS films and were ultrasonically cleaned before deposition. The substrate temperature was monitored by a chromel–alumel thermocouple, which was attached to the front surface of the substrate holder. Evaporation was carried out by varying the substrate temperature from 100 to 300 °C.

X-ray diffraction patterns and optical transmission spectra were obtained using a Fangyuan X-ray diffractometer (DX-2000) and a Shimadzu UV-vis spectrophotometer (UV-2450), respectively. The X-ray diffractometer was operated at 40 kV and 25 mA with CuK $\alpha$  radiation of wavelength 1.5406 Å. Transmission spectra were recorded in the range of 190–800 nm. The photoluminescence analysis of the films was performed using a Hitachi Fluorescence Spectrophotometer (FL-7000). The thickness of the films was measured by employing a profilometer (KLA Tencor  $\alpha$ -step-500).

## 3. Results and discussion

### 3.1. Structural analysis

Figure 1 shows the XRD patterns of the CdS films grown by the electron beam evaporation technique. The diffraction

\* Project supported by the National Natural Science Foundation of China (No. 50902012) and the Research Foundation of the Chengdu University of Information Technology, China (No. CRF200924).

<sup>†</sup> Corresponding author. Email: ydy\_lz@sohu.com

Received 8 July 2010, revised manuscript received 27 September 2010

© 2011 Chinese Institute of Electronics

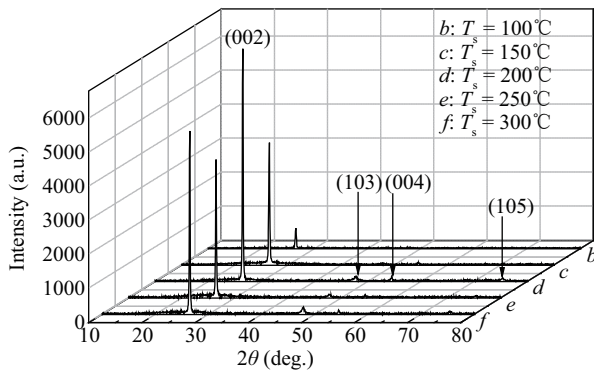


Fig. 1. XRD patterns of CdS films deposited at different substrate temperatures ( $T_s$ ).

Table 1. Structural parameters of the CdS films (thickness ( $t$ ),  $2\theta$  and d-spacings ( $d$ ) of (002) plane, calculated preferential orientation factor  $f(002)$ , grain size ( $D$ ), dislocation density ( $\delta$ ) and film stress ( $\xi$ ).

$T_s$ (°C)	$t$ (nm)	$2\theta$	$d$ (Å)	$f(002)$	$D$ (nm)	$\delta$ ( $10^{14}$ line/m <sup>2</sup> )	$\xi$ ( $10^{-4}$ )
100	1124	26.512	3.3592	0.9669	34.4	8.451	9.301
150	982	26.502	3.3604	0.9592	36.9	7.344	8.322
200	583	26.504	3.3602	0.8788	45.8	4.767	7.346
250	410	26.467	3.3648	0.8897	43.7	5.236	7.221
300	194	26.498	3.3610	0.8338	44.4	4.645	7.091

peaks show that they have a polycrystalline structure of hexagonal phase, with a (002) preferred orientation. The structural parameters of the CdS films deposited at different substrate temperatures ( $T_s$ ) were calculated and are given in Table 1. Also, the measured film thickness ( $t$ ), observed  $2\theta$  and d-spacings ( $d$ ) of the (002) plane of all the samples are listed in Table 1. The preferred orientation factor  $f(hkl)$  of the prominent peaks of the prepared CdS films has been obtained by evaluating the fraction of the intensity of that particular plane over the sum of the intensities of all the peaks within a given  $2\theta$  range ( $10^\circ$ – $80^\circ$ ). The preferential orientation factor of the (002) plane of samples deposited at low substrate temperature is very large (0.9669) when compared with samples grown at a higher temperature (0.8338 at 300 °C). The increasing substrate temperature promoted the growth of other crystal planes, such as (103), (004) and (105), which decreased the preferential orientation factor of the (002) plane. Overall, large values of the (002) preferential orientation factor indicate a strong orientational growth along the (002) plane.

The grain size ( $D$ ) values are calculated using the Scherrer formula<sup>[8]</sup>,

$$D = \frac{0.9\lambda}{\beta \cos \theta}, \quad (1)$$

where  $\lambda$  is the wavelength of the X-ray diffraction used (1.5406 Å),  $\beta$  is the full-width at half-maximum (FWHM) of the peak which has maximum intensity and  $\theta$  is the Bragg angle. The dislocation density ( $\delta$ ), defined as the length of dislocation lines per unit volume, has been estimated using the equation<sup>[9]</sup>

$$\delta = \frac{1}{D^2}, \quad (2)$$

where  $\delta$  is the measure of the amount of defects in a crystal.

Therefore, the small values of  $\delta$  indicate the good crystallinity of the CdS films. Finally, the stress ( $\xi$ ) of the films was determined with the use of the following formula,

$$\xi = \frac{\beta \cos \theta}{4}. \quad (3)$$

The differences in thermal expansion coefficients and lattice constants between the film and the substrate causes mechanical stress, resulting in film instability or even peeling. Therefore, it is an important step in film deposition to reduce the film stress, which usually can be done by raising the substrate temperature or through film annealing.

It can be seen from Table 1 that the grain size increases gradually with increasing substrate temperature and reaches its maximum of 45.8 nm at 200 °C. However, the grain size decreases as the substrate temperature further improves. The same trend is also observed in the XRD patterns of CdS films, as seen in Fig. 1. It is generally believed that the surface migration of adsorbed particles on substrates increases with the increasing substrate temperature and is of benefit to grain growth and crystalline quality. However, higher temperatures also lead to an increased desorption rate of adsorbed particles, and then decreases the film thickness, as shown in Table 1. It is found that there actually exists an optimal film thickness in the growth of thin films, and as the film thickness is less than this value, the growth of film grain is not sufficient. On the other hand, the film’s roughness increases when the thickness exceeds this critical value, and then the migration of subsequently adsorbed particles is reduced greatly, resulting in lower crystalline quality, such as the powder phenomenon on the film surface. Therefore, controlling growth temperature and film thickness to appropriate levels is a key step for the preparation of high quality thin films.

### 3.2. Optical analysis

Figure 2 shows the transmission curves of CdS films deposited at different temperatures. It can be found that the absorption edge of the films becomes steeper and present high transmission (65%–95%) in the visible range with increasing substrate temperature. The oscillatory nature of the transmission spectra observed for all of the films is attributed to the interference of light transmitted through the thin film and the substrate. According to the related theories of semiconductor materials, the relation connecting the absorption coefficient  $\alpha$ , the incident photon energy  $h\nu$  and optical band gap  $E_g$  obey the following equation<sup>[10]</sup>,

$$(\alpha h\nu)^n = B(h\nu - E_g), \quad (4)$$

where  $B$  is a constant, for direct transition materials,  $n = 2$ . The band gap of CdS films deposited at different temperatures was determined by extrapolating the linear portion of the  $(\alpha h\nu)^2$  versus  $h\nu$  plots to the energy axis, shown in Fig. 3. The estimated  $E_g$  values in the range of 2.389–2.448 eV were presented in Table 2.

As shown in Fig. 3, the absorption curve of CdS films presents a trailing phenomenon along the direction of low photon energy, that is an Urbach tail<sup>[11]</sup>. It is generally believed that the band tail near the bottom of the conduction band, which

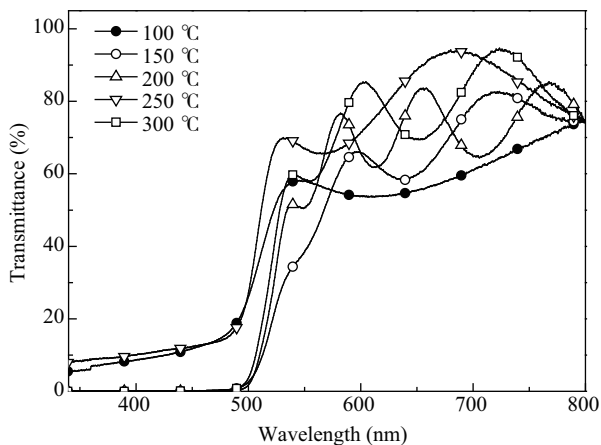


Fig. 2. Optical transmittance spectra of CdS films as a function of wavelength for the samples deposited at different substrate temperatures.

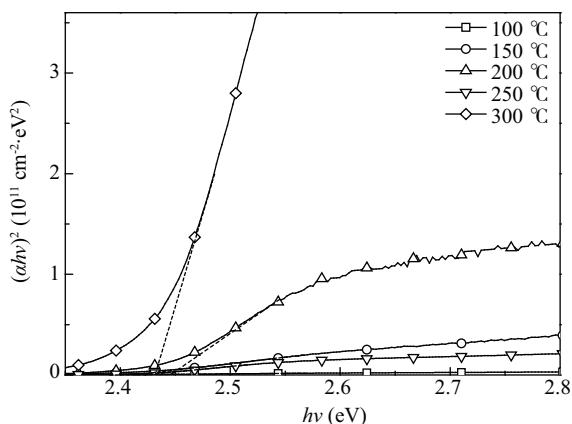


Fig. 3.  $(\alpha hv)^2$  versus  $h\nu$  plot of CdS films deposited at different substrate temperatures.

Table 2. Optical parameters of the CdS films (band gap ( $E_g$ ) and tail width ( $\Delta$ )).

$T_s$ (°C)	100	150	200	250	300
$E_g$ (eV)	2.389	2.416	2.448	2.422	2.436
$\Delta$ (eV)	0.158	0.117	0.093	0.082	0.079

originated from the disordered structure of films, is responsible for the Urbach tail, resulting in an extension of UV-vis transmittance spectra to the low energy side. Moreover, the density of the disordered structure of films is usually qualitatively analyzed by calculating the tail width. The relation of absorption coefficient  $\alpha$  of the Urbach tail and the photon energy  $h\nu$  is represented by the following formula,

$$\ln \alpha = \frac{h\nu}{\Delta} + C, \quad (5)$$

where  $C$  is a constant and  $\Delta$  is the band tail width. The  $\ln \alpha$  versus  $h\nu$  plot is linear near the absorption edge, and it is possible to infer the tail width of the films by the slope of the straight line portion of this plot, shown in Fig. 4. The tail width in the range of 0.079–0.158 eV is also presented in Table 2.

It is found from Table 2 that the band gap of CdS films

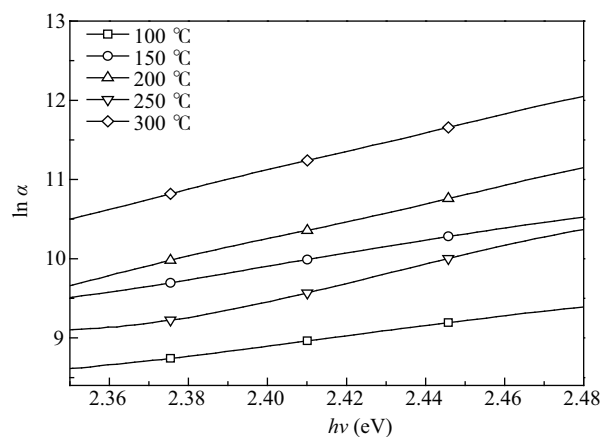


Fig. 4. Variation of  $\ln \alpha$  versus  $h\nu$  for samples deposited at different substrate temperature.

increased from 2.389 to 2.448 eV when the substrate temperature increases from 100 to 200 °C, then decreased to 2.422 eV at 250 °C, but increased to 2.436 eV once again at 300 °C. Meanwhile, the tail width of CdS films decreased monotonically with the increase in substrate temperature due to the improvement in crystalline quality of prepared films, resulting in the decrease in the band gap. However, the stoichiometry of CdS films changed by the fact that the sticking coefficients of Cd, S and CdS vary with the substrate temperature. The sticking coefficient of Cd decreases as the substrate temperature increases<sup>[12]</sup>. So, the stoichiometry of the CdS films changes from a more Cd-rich composition to a less Cd-rich composition. As a result, the band gap increases as the substrate temperature rises. Accordingly, attributed to the opposite influence of tail width and Cd-composition to the band gap of CdS films, the band gap exhibits fluctuation changes with increases in substrate temperature.

The photoluminescent (PL) spectra of the CdS films deposited at different substrate temperatures, as shown in Fig. 5, was measured at room temperature in which the excitation wavelength of 390 nm is chosen for samples. Usually, the as-deposited CdS films only show weak luminescence at room temperature due to the non-radiative defects with energy levels near the midgap. It is found that the PL peak of samples is around 1.60 eV (red emission), regardless of substrate temperature. The red band observed in CdS photoluminescence spectra is ascribed to the transition of bound electrons from surface states (such as surface Cd-vacancy) to the valence band<sup>[13]</sup>. In our case, the only weak red band is more likely to originate from the transition of Cd-vacancy acceptors to the valence band. This means that these samples were cadmium-poor. As the substrate temperature increases from 200 to 300 °C, the peak position of the red bands shifted little but the intensity increased slightly with increasing substrate temperature. As explained above, the Cd-composition of the CdS films decreased as the substrate temperature increased, resulting in an increased concentration of Cd-vacancy. Consequently, the intensity of red emission increased. In polycrystalline systems, the PL emission lines are not sharp peaks but are broad bands because of the presence of many recombination sites; the grains will have different impurity concentrations, surface areas and

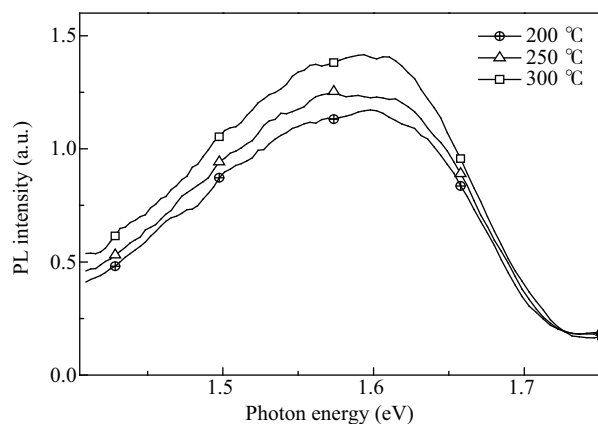


Fig. 5. Photoluminescence spectra of CdS films deposited at different substrate temperatures.

defect types and concentrations (e.g. stacking faults)<sup>[4]</sup>.

#### 4. Conclusion

CdS films deposited by electron beam evaporation are shown to have a polycrystalline hexagonal phase and exhibited preferred orientation along the (002) plane. Due to enhancement of the nucleation rate and migration ability of adsorbed CdS particles as the substrate temperature increased, the crystalline quality of the CdS films improved first. However, further increasing the substrate temperature reduced the film thickness, leading to a lower crystalline quality. So, it is important to control the growth temperature and film thickness to an appropriate value for the preparation of high quality thin films. It is found that the optical band gap of the CdS films exhibited fluctuation changes with increasing substrate temperature, and was attributed to the variation in Cd-composition and density of the disorder structure in the samples. Moreover, the red emission peak of the CdS films in PL spectra was observed,

which probably originates from transitions of Cd-vacancy acceptors to the valence band.

#### References

- [1] Shay J L, Wagner S, Kasper H M. Efficient CuInSe<sub>2</sub>/CdS solar cells. *Appl Phys Lett*, 1975, 27: 89
- [2] Krishnan S, Sanjeevb G, Pattabi M, et al. Effect of electron irradiation on the properties of CdTe/CdS solar cells. *Solar Energy Materials and Solar Cells*, 2009, 93: 2
- [3] Iacomi F, Purica M, Budianu E, et al. Structural studies on some doped CdS thin films deposited by thermal evaporation. *Thin Solid Films*, 2007, 515: 6080
- [4] Lee J H, Lee D J. Effects of CdCl<sub>2</sub> treatment on the properties of CdS films prepared by r.f. magnetron sputtering. *Thin Solid Films*, 2007, 515: 6055
- [5] Badera N, Godbole B, Srivastava S B, et al. Quenching of photoconductivity in Fe doped CdS thin films prepared by spray pyrolysis technique. *Appl Surf Sci*, 2008, 254: 7042
- [6] Rakhshani A E, Al-Azab A S. Characterization of CdS films prepared by chemical-bath deposition. *J Phys: Condensed Matter*, 2000, 12: 8745
- [7] Sasikala G, Thilakan P, Subramanian C. Growth and characterization of CdS semiconducting thin films for photovoltaic applications. *Solar Energy Materials and Solar Cells*, 2000, 62: 275
- [8] Atay F, Bilgin V, Akyuz I, et al. The effect of In doping on some physical properties of CdS films. *Mater Sci Semicond Processing*, 2003, 6: 197
- [9] Prabahaar S, Dhanam M. CdS thin films from two different chemical baths-structural and optical analysis. *J Cryst Growth*, 2005, 285: 41
- [10] Tauc J. *Amorphous and liquid semiconductors*. New York: Plenum Press, 1975
- [11] Urbach F. The long-wavelength edge of photographic sensitivity and of the electronic absorption of solids. *Phys Rev*, 1953, 92: 1324
- [12] Wilson J I B, Woods J. The electrical properties of evaporated films of cadmium sulphide. *J Phys Chem Solids*, 1973, 34: 171
- [13] Goto F, Shirai K, Ichimura M. Defect reduction in electrochemically deposited CdS thin films by annealing in O<sub>2</sub>. *Solar Energy Materials and Solar Cells*, 1998, 50: 147